Carbon nanotube-based quantum spin pump

2006 New J. Phys. 8 73

(http://iopscience.iop.org/1367-2630/8/5/073)

New Journal of Physics
The open-access journal for physics

Carbon nanotube-based quantum spin pump

Yunjin Yu[1,2], **Yadong Wei**[2] **and Jian Wang**[3,4]

[1] Key Laboratory of Materials Physics, Institute of Solid State Physics, Chinese Academy of Sciences, Hefei 230031, People's Republic of China
[2] Department of Physics, School of Science, Shenzhen University, Shenzhen 518060, People's Republic of China
[3] Department of Physics and the Center of Theoretical and Computational Physics, The University of Hong Kong, Pokfulam Road, Hong Kong, People's Republic of China
E-mail: jianwang@hkusua.hku.hk

New Journal of Physics **8** (2006) 73
Received 20 January 2006
Published 25 May 2006
Online at http://www.njp.org/
doi:10.1088/1367-2630/8/5/073

Abstract. By cyclic variation of the magnetic field and electric field, we investigate the spin current of a carbon nanotube-based molecular quantum spin pump. At finite frequencies, we calculate the spin current to the second order in pumping amplitudes. In the presence of the magnetic field, a pure spin current without accompanying charge current is generated at zero bias voltage. The photon-assisted process is clearly observed in the spin current.

Recently, there has been a growing interest in the field of spintronics, especially the physics of quantum spin transport [1]. Spintronic devices have promising potential applications because of longer coherent lifetime, faster data processing speed and lower energy dissipation [2]. The primary concerns focus on the generation of the pure spin current and its manipulation and detection and finally the manufacture of spintronic devices. In order to get a spin battery device that generates spin current without accompanying charge current, many quantum systems that are based on magnetic semiconductors [3, 4], ferromagnetic metals [5], ferromagnetic resonance devices [6, 7] and spin-dependent pumps [8]–[30] have been investigated. Among them, the spin pumping method is most interesting because it can serve as a spin battery. Since the principle of the quantum parametric pump was proposed by Thouless [31], it has attracted great attention [32]–[46]. The spin polarized pump has also been theoretically studied and experimentally realized. To design a spin pump, various structures with different pumping methods have been proposed. Such structures include: open quantum dot [9, 13, 15], nearly closed quantum dot [27] coupled with normal metal leads in a magnetic field, open quantum dot pump in the presence of a ferromagnetic

[4] Author to whom any correspondence should be addressed.

PII: S1367-2630(06)17165-7

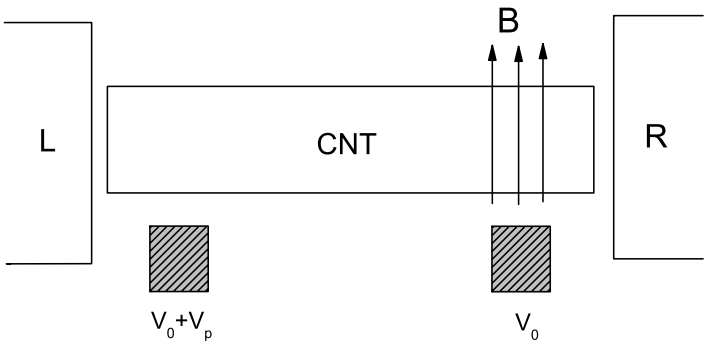

Figure 1. A schematic plot of a N-CNT-N pumping device driven by an electric field and a magnetic field simultaneously.

lead [14] or in the presence of a superconducting lead [22], ac-driven double quantum dots in the Coulomb blockade regime [25], the carbon nanotube (CNT)-based quantum pump in the presence of a magnetic field [19], an interacting quantum wire in the Luttinger liquid regime [16], three-terminal ferromagnet–superconductor–semiconductor structure based on the crossed normal/Andreev reflection [23, 30]. Apart from applying the time-dependent electric potential, the time-dependent magnetic barriers [8, 17], the rotating magnetic moment or rotating external magnetic field [7, 10, 22], the oscillating magnetic field [15], and shining microwave in the presence of non-uniform magnetic field [12] are also used as driving forces to generate the spin current. Finally, the spin–orbit-based (see [47] or [48]) quantum pump [11, 17, 20, 29] was also found to be a possible method to obtain pure spin current. In this paper, we investigate the generation of a pure spin current using the idea of parametric pumping. In the absence of a spin flip mechanism, the spin current can be defined as the particle current multiplied by the electron spin $\pm\hbar/2$. A pure spin current is produced if an electron with up spin traverses to the left lead while an electron with down spin goes to the right lead so that the total charge current is zero and the net spin current is nonzero. It is well known that the charge is coupled by the electric field and the spin of electron is coupled by the magnetic field. As a result, to drive a spin current, a time-dependent magnetic stripe field can be used as one of the driving forces. Actually, when the magnetic field is present in the lead, the spin-up electron is positively biased and the spin-down electron is negatively biased. Hence a spin current may be produced. This idea can be similarly applied in parametric pumping when the external bias is zero while the system is parametric such that an external magnetic field inside the device is nonzero [13].

The system we studied is a finite CNT coupled with external leads. Since the original discovery of the CNT, it has been intensively studied both experimentally and theoretically [49]–[57]. The CNT-based parametric electron pump has been investigated as a prototypical nanometre-scale molecular device [40, 46]. Due to the peculiar electronic properties of CNTs [51]–[55], the CNT-based quantum electron pump shows antisymmetric pumped signals near the many doubly degenerate resonant levels of the finite-length CNT for a wide range of energies [40]. The schematic plot of the device that we used is plotted in figure 1. Two metallic gates with the same electric potential $V_{10} = V_{20} = V_0 = 2.7$ eV are placed near two ends of the CNT between $0.1L$ to $0.3L$ (region I) and between $0.7L$ to $0.9L$ (region II). Hence, our system is a symmetric open system.[5] To generate spin current, two driving forces, one is

[5] For an asymmetric system, the current can be pumped by illuminating an ac field, see [58].

the oscillating electric potential $V_{\rm I} = V_p \cos(\omega t)$ with frequency ω and another is due to the oscillating magnetic field $V_{{\rm II}\sigma} = \sigma\mu_B B(t) = \sigma\mu_B B_0 \cos(\omega t + \phi)$ with a phase difference ϕ, are added in the scattering region I and region II, respectively. The magnetic field is along the z-direction which is perpendicular to the axis of the CNT (see figure 1), i.e., $\mathbf{B} = B(t)\hat{z}$. Finally, the Hamiltonian due to the time-varying parameters can be written as:

$$H'_\sigma(t) = \sum_{\rm I} V_{\rm I}\Delta_{\rm I} + \sum_{\rm II} V_{{\rm II}\sigma}\Delta_{\rm II}. \tag{1}$$

Here $\sigma = \pm 1$ for spin $\uparrow\downarrow$, Δ_i is the potential profile and is set to unity for the region near the gate and zero otherwise. To simplify the discussion, we neglect the spin flip due to the spin relaxation mechanism. We have also neglected the possible spin–orbit coupling in our calculation.

Without considering the interaction of electrons in the ideal leads, we start from the standard non-equilibrium Green function expression for the average particle current in the left lead

$$I_{\rm L} = -\frac{1}{\tau}\int_0^\tau {\rm d}t \int {\rm d}t_1 {\rm Tr}[\mathbf{G}^r(t,t_1)\mathbf{\Sigma}^<_{\rm L}(t_1,t) + \mathbf{G}^<(t,t_1)\mathbf{\Sigma}^a_{\rm L}(t_1,t) + {\rm c.c.}], \tag{2}$$

where $\tau = 2\pi/\omega$ is the period of cyclic variation. $\mathbf{G}^r$,$\mathbf{G}^<$ is the 2×2 retarded Green function and the less Green function in spin space. $\mathbf{\Sigma}_{\rm L(R)}$ is the self-energy due to the interaction of the conductor and the left (right) lead modelled using the line width function $\Gamma_{\rm L(R)}$ [59]. In our calculation, the wide band limit is used and the related line width function is assumed to be spin independent.

In general, a perturbation theory is needed to solve a time-dependent problem [41]. By using the Dyson equation in spin space, the retarded Green function can be expressed as

$$\mathbf{G}^r(t,t') = \mathbf{G}^{0r}(t-t') + \int {\rm d}t_x\, \mathbf{G}^{0r}(t-t_x)\mathbf{H}'(t_x)\mathbf{G}^{0r}(t_x - t\prime) + \cdots. \tag{3}$$

If we neglect the spin flip during the pumping process, $\mathbf{H}'(t)$ will be a diagonal matrix with $H'_\sigma(t)$ (see equation (1)) the diagonal matrix elements. $\mathbf{G}^{0r}(t,t') = \mathbf{G}^{0r}(t-t')$ is the Green function in the absence of $\mathbf{H}'$. So it is also the diagonal matrix and its two diagonal matrix elements for spin up and spin down are the same. In this paper, we only consider the small driving forces and calculate the retarded Green function up to the first order of the pumping amplitudes. Hence, the corresponding average current is up to the second order of the pumping amplitudes.

We extend the integration range of dt in equation (2) to $[-N\tau, N\tau]$ with $N \to \infty$. By taking a double-time Fourier transform, we obtain the following result:

$$I_{\rm L} = -\frac{1}{2N\tau}\int \frac{{\rm d}E\,{\rm d}E'}{(2\pi)^2}{\rm Tr}[\{(\mathbf{\Sigma}^r_{\rm L}(E) - \mathbf{\Sigma}^a_{\rm L}(E))\mathbf{G}^r(E,E')\mathbf{\Sigma}^<(E') - \mathbf{\Sigma}^<_{\rm L}(E)\mathbf{G}^r(E,E')(\mathbf{\Sigma}^r(E') - \mathbf{\Sigma}^a(E'))\}\mathbf{G}^a(E',E)]. \tag{4}$$

After some algebra and expanding the Green function up to the first order of the pumping amplitudes, the pumped particle current can be obtained at finite frequency and up to the second order in pumping amplitudes as [42] ($\hbar = 1$)

$$I_{\rm L} = \sum_{\sigma=-1,1} I_{{\rm L}\sigma}, \tag{5}$$

with

$$I_{\mathrm{L}\sigma} = I_{11} + \sigma I_{12} + \sigma I_{21} + I_{22}, \tag{6}$$

where

$$I_{11} = \frac{\mathrm{i}V_1^2}{8\pi}\int \mathrm{d}E \sum_{jj'} \Gamma_{\mathrm{L}} G^{0r}_{\mathrm{L}j}[(f^- - f)(G^{0r-}_{jj'} - G^{0a-}_{jj'}) + (f^+ - f)(G^{0r+}_{jj'} - G^{0a+}_{jj'})]G^{0a}_{j'\mathrm{L}}, \tag{7}$$

$$I_{12} = \frac{\mathrm{i}V_1V_2}{8\pi}\int \mathrm{d}E \sum_{jm} \Gamma_{\mathrm{L}} G^{0r}_{\mathrm{L}j}[(f^- - f)(G^{0r-}_{jm} - G^{0a-}_{jm})\mathrm{e}^{\mathrm{i}\phi} + (f^+ - f)(G^{0r+}_{jm} - G^{0a+}_{jm})e^{-\mathrm{i}\phi}]G^{0a}_{m\mathrm{L}}, \tag{8}$$

$$I_{21} = \frac{\mathrm{i}V_2V_1}{8\pi}\int \mathrm{d}E \sum_{jm} \Gamma_{\mathrm{L}} G^{0r}_{\mathrm{L}m}[(f^- - f)(G^{0r-}_{mj} - G^{0a-}_{mj})\mathrm{e}^{-\mathrm{i}\phi} + (f^+ - f)(G^{0r+}_{mj} - G^{0a+}_{mj})\mathrm{e}^{\mathrm{i}\phi}]G^{0a}_{j\mathrm{L}}, \tag{9}$$

$$I_{22} = \frac{\mathrm{i}V_2^2}{8\pi}\int \mathrm{d}E \sum_{mm'} \Gamma_{\mathrm{L}} G^{0r}_{\mathrm{L}m}[(f^- - f)(G^{0r-}_{mm'} - G^{0a-}_{mm'}) + (f^+ - f)(G^{0r+}_{mm'} - G^{0a+}_{mm'})]G^{0a}_{m'\mathrm{L}}, \tag{10}$$

where $f^{\pm} = f(E \pm w)$ is the Fermi distribution function, $G^{0r\pm} = G^{0r}(E \pm w)$ is the diagonal element of the Green function $\mathbf{G}^{0r}(E)$ when the driving parameters are zero. In the above equations, indices j and j' belong to region I and indices m and m' belong to region II. For simplicity, we set $V_1 = qV_p$ and $V_2 = \mu_B B_0$. Physically, the terms with $f^- = f(E - w)$ present the photon-absorption process and the terms with $f^+ = f(E + w)$ correspond to the photon-emission process. In the calculation below, we set $\phi = \pi/2$.

From (7)–(10), we obtain the spin-up particle current

$$I_{L\uparrow} = I_{11} + I_{12} + I_{21} + I_{22}, \tag{11}$$

and the spin-down particle current is given by

$$I_{\mathrm{L}\downarrow} = I_{11} - I_{12} - I_{21} + I_{22}. \tag{12}$$

So the total charge current is

$$I_{\mathrm{e}} = q(I_{\mathrm{L}\uparrow} + I_{\mathrm{L}\downarrow}) = 2q(I_{11} + I_{22}), \tag{13}$$

and the total spin current is

$$I_{\mathrm{s}} = \tfrac{1}{2}\hbar(I_{\mathrm{L}\uparrow} - I_{\mathrm{L}\downarrow}) = \hbar(I_{12} + I_{21}). \tag{14}$$

Now we consider a (5, 5) armchair CNT with 200 unit cells of carbon atoms (total 4000 atoms). We specifically consider situations where the nanotube is well contacted with the electrodes and therefore transport is not in the Coulomb blockade regime. To do that, we apply the wideband limit [59] by fixing the coupling between CNT and electrode $\Gamma_{\mathrm{L}} = \Gamma_{\mathrm{R}} = 3.4$ eV to make the device transparent during the pumping process. The value of Γ can also be calculated accurately using *ab initio* techniques [60]. The CNT is modelled by the nearest-neighbour π-orbital tight-binding approach with the bond potential $V_{pp\pi} = -2.75$ eV for the carbon atoms. This tight-binding model is known to give a reasonable, qualitative description of the

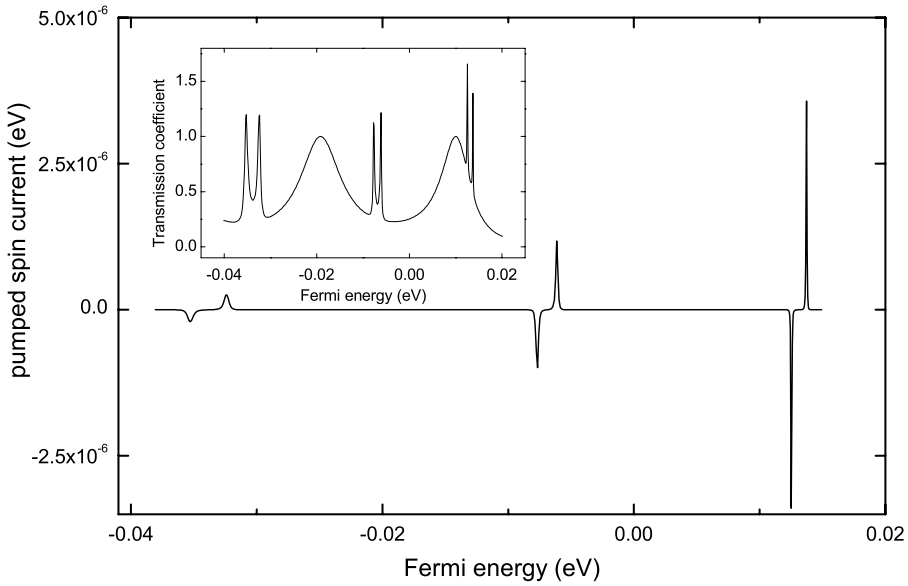

Figure 2. The total pumped spin current versus Fermi energy with $V_0 = 2.72$ eV, $V_1 = 0.0005$ eV, $V_2 = 0.0005$ eV, $\omega = 10^9$ Hz and $\phi = \pi/2$. Inset: the transmission coefficient versus Fermi energy.

electronic and transport properties of CNTs [61]. We note that there are many experimental data suggesting that Coulomb interaction in CNTs [53, 62] can be very important and Luttinger liquid theory [8] leads to new and interesting physics. There are still many experimental results showing various physical phenomena for which single electron theory is adequate.

In figure 2, we plot the total pumped spin current and total pumped charge current as a function of the Fermi energy at zero temperature. For comparison, we also plot the static transmission coefficient as a function of the Fermi energy in the inset of figure 2. For the static case, where driving forces are zero, the finite-sized CNT energy spectrum has many doubly degenerate levels. When the CNT is in contact with external leads, these degenerate levels split, resulting in resonance pairs (see inset of figure 2). From figure 2, the following observations are in order. First of all, since the spin current is generated in the absence of external bias, our device can be used as a spin battery. This happens in the symmetric case ($V_1 = V_2$ and $\Gamma_L = \Gamma_R$). To the second order of driving forces the total pumped charge current is zero, so the pure spin current can be obtained. To understand the physics behind this, we plot I_{11} and I_{22} as a function of Fermi energy in figure 3. We find that I_{11} and I_{22} have the same value but with opposite sign. Actually, if we set $V_1 = 0$, $V_2 \neq 0$ or $V_1 \neq 0$, $V_2 = 0$ in (6), we will only get I_{22} or I_{11} which is due to the single parameter pumping effect. If the pumping system with single parameter V_1 (see the upper inset of figure 3) is symmetric to the system with single parameter V_2 (see the lower inset of figure 3) and the pumping driving forces have the same strength (let V_1 and V_2 have the same value), they will give the same pumped particle current but in opposite direction. We can also start from (7) and (10) to confirm it. By assuming $\Gamma_L = \Gamma_R$ and $H(i, j) = H(N + 1 - j, N + 1 - i)$ (N is the dimension of the Hamiltonian), we can get $I_{11} = -I_{22}$ exactly. Second, we see that the pumped spin current is at the Fermi energies where the transmission coefficient has a very sharp peak. We have confirmed that the sharp peaks of transmission coefficient occur at energies where there are very large scattering total density of states (DOS), while the broad peaks are at

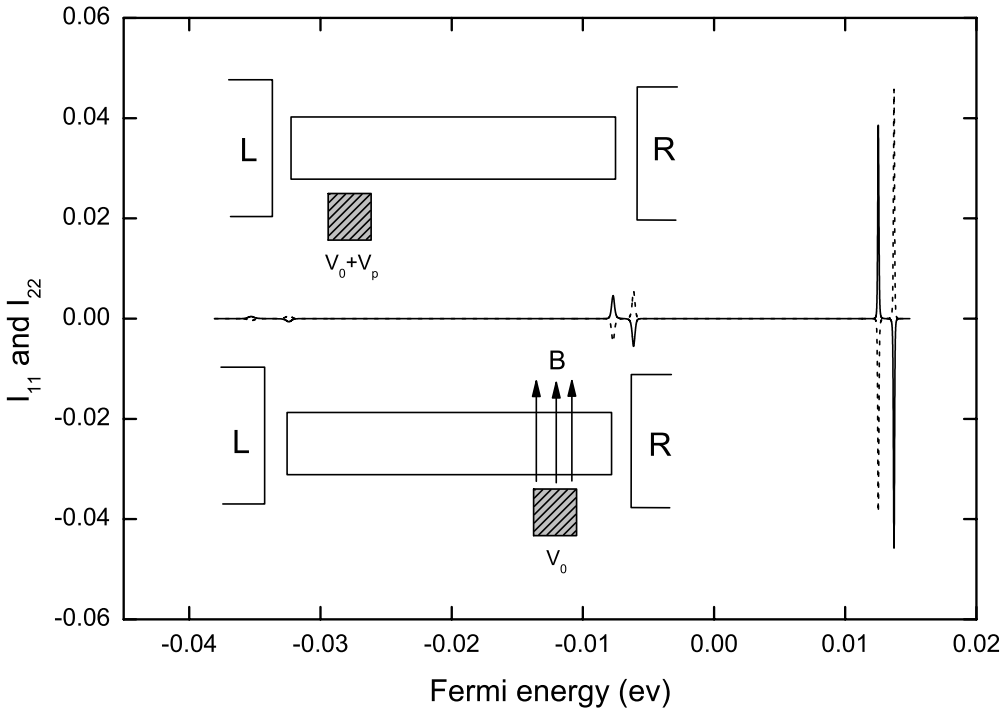

Figure 3. The pumped particle current terms of I_{11}(———) and I_{22}(· · · · · ·) versus Fermi energy. The parameters are the same as those in figure 2. Upper and lower insets are schematic plots for the single parametric pump driven by electric field or magnetic field respectively.

energies characterized by small total DOS. The sharp transmission peaks are usually grouped in pairs where the spin pump current occurs. The results clearly show that the pumped spin current is assisted by the resonant energy levels. Third, to the second order of the pumping amplitudes, the pure spin current occurs for any Fermi energy so that the pure spin current can be obtained without tuning the Fermi energy. Fourth, for different Fermi energies, the pumped spin current can be driven either from the left lead to the right lead or vice versa depending on the system parameters. For parametric pumping, the external bias voltage is zero. Hence, the magnitude and the direction of the current are very sensitive to various parameters of the system such as potential landscape of the pump [63], frequency of the driving force [42], and Fermi energy of the leads [64]. Hence, the spin current reversal is a generic feature of the parametric pump. We wish to emphasize that what we have studied here is a non-adiabatic spin pump for a molecular device up to the second order in pumping amplitudes. Hence, the pumping amplitude should be small. Although the same frequency of the electric field and the magnetic field have been used, they are not necessarily the same. We also found that when the temperature is increased to 5 K the sharp peaks shown in figure 2 will become flat and the peak height will be about 13% of the original ones.

We now investigate the pumped spin current as a function of frequencies. In figure 4, we plot the pumped spin current as a function of pumping frequency at different Fermi energies. First, let us examine figure 4(a) which is plotted at $E_f = -0.00615$ eV so that E_f is in line with one of the two pairing resonant levels at $E_1 = -0.00768$ eV and $E_2 = -0.00615$ eV

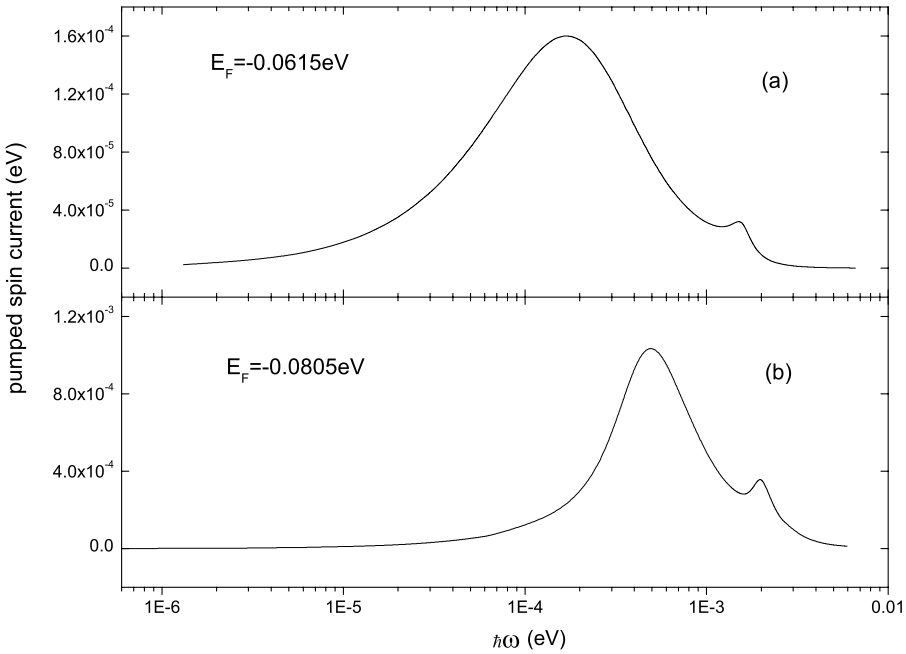

Figure 4. The pumped spin current versus the pumping frequency at (a) $E_f = -0.00615$ eV and (b) $E_f = -0.00805$ eV. The other parameters are the same as those in figure 2.

(see the middle pairing levels of the inset of figure 2). We find that when the pumping frequency is smaller than $\hbar\omega = 10^{-5}$ eV, the pumped spin current increases almost linearly with the pumping frequency. In the nonlinear regime the spin current increases quickly with the frequency. After the spin current arrives at its maximum point at $\hbar\omega = 1.7 \times 10^{-4}$ eV, it begins to decrease with frequency. We can clearly find another spin current peak with much smaller peak height at $\hbar\omega = 0.00154$ eV and the difference between the E_f and E_1 is also very close to the frequency ($E_f - E_1 = 0.00153$ eV). This is clearly a photon-assisted process. The electron with energy E_f emits a photon and leaves the system with energy E_1. To confirm this picture, we carry out the calculation at $E_f = -0.00805$ eV again and plot the data in figure 4(b). There are two spin current peaks located at $\hbar\omega \simeq E_1 - E_f = 0.00037$ eV and $\hbar\omega \simeq E_2 - E_f = 0.00019$ eV. It shows that the electron with energy E_f absorbs a photon and is pumped out at the energy level E_1 or E_2. The highest pumping frequency we used in figure 4 is of the order of THz.[6] For the parametric pumping, the previous experiments have been realized in the frequency regime 10^8 Hz [33]. It would be a challenge for experimentalist to reach the frequency in the THz regime for the parametric pumping. However, there do exist some ac experiments with frequencies that are close to THz. For instance, oscillation up to 712 GHz has been achieved in InAs/AlSb resonant tunnelling diodes [65]. For nano-structures, most recently Rosenblatt [66] has demonstrated a single-walled CNT transistor operated at frequencies up to 50 GHz. We note that in the high-frequency regime, the oscillating electric field can induce a magnetic field and vice versa. These induced electric and magnetic fields may affect our result. For the frequency regime and the

[6] The frequency ω in our paper is angular frequency which is related to the frequency ν that experimentalist used through $\omega = 2\pi\nu$.

sample size we have studied here, we can reasonably neglect the induced electric field.[7] Another challenge for experimentalists would be to measure the pumped spin current. So far at least three methods are proposed in the literature. (i) The anomalous Hall effect [67] can be used to detect the spin current. In this method, a spin current polarized perpendicular to the 2DEG can lead to an anomalous Hall voltage across the sample [67]. (ii) One can also use spin current induced electric field [68] to get a spin signal. (iii) Recently, another method has been proposed and realized by Folk *et al* [69] using a gate-controlled bidirectional spin filter. With this technique, the measurement of spin current is experimentally feasible [69]. Finally, efficient spin injection from the 'spin battery' to the spin devices is also an important issue [70].

To summarize, we have investigated the CNT-based molecular quantum spin pump at finite frequency up to the second order in pumping amplitude. Apart from the electric potential, the magnetic field is used as one of the driving forces. The pure spin current is obtained for a wide range of Fermi energy. By adjusting the Fermi energy, the spin current can switch its direction. The photon-assisted process is clearly seen as the driving frequency changes. It is confirmed that such a device may be used as one kind of spin battery.

Acknowledgments

We gratefully acknowledge support by a RGC grant from the SAR Government of Hong Kong under grant number HKU 7044/05P, the CRCG grant from The University of Hong Kong, the grant from NSFC under grant number 10574093 (to YW). Some of the calculations were performed at the Center for Computational Science, Hefei Institute of Physical Science.

References

[1] Prinz G A 1998 *Science* **282** 1660
Wolf S A *et al* 2001 *Science* **294** 1488
[2] Kikkawa J M and Awschalom D D 1999 *Nature* **397** 139
[3] Fiederling R *et al* 1999 *Nature* **402** 787
[4] Ohno Y *et al* 1999 *Nature* **402** 790
[5] Zhu H J *et al* 2001 *Phys. Rev. Lett.* **87** 016601
[6] Brataas A *et al* 2002 *Phys. Rev.* B **66** 060404
[7] Tserkovnyak Y *et al* 2002 *Phys. Rev.* B **66** 224403
[8] Sharma P and Chamon C 2001 *Phys. Rev. Lett.* **87** 096401
[9] Mucciolo E R *et al* 2002 *Phys. Rev. Lett.* **89** 146802
[10] Wang B G *et al* 2003 *Phys. Rev.* B **67** 092408
[11] Sharma P and Brouwer P W 2003 *Phys. Rev. Lett.* **91** 166801
[12] Sun Q F *et al* 2003 *Phys. Rev. Lett.* **90** 258301
[13] Watson S K *et al* 2003 *Phys. Rev. Lett.* **91** 258301
[14] Zheng W *et al* 2003 *Phys. Rev.* B **68** 113306
[15] Aono T 2003 *Phys. Rev.* B **67** 155303

[7] To estimate the electromotive force ε generated by the time-dependent magnetic field, we use Faraday's law: $\varepsilon = -\int \frac{\partial \mathbf{B}}{\partial t} \cdot \mathrm{d}\mathbf{S}$ or $\varepsilon \sim \pi r^2 \omega B$, where r measures size of the region of the time-dependent magnetic field. If we take $r \sim 10$ nm, $B \sim 1$ T and $\omega \sim 10^{10}$ Hz, we find $\varepsilon \sim 1$ μeV which is two orders of magnitude smaller than the pumping electric field we used.

[16] Citro R *et al* 2003 *Phys. Rev.* B **68** 165312
[17] Benjamin R and Benjamin C 2004 *Phys. Rev.* B **69** 085318
[18] Wang B G *et al* 2004 *Phys. Rev.* B **69** 153301
[19] Wei Y D *et al* 2004 *Phys. Rev.* B **70** 045418
[20] Zhou F 2004 *Phys. Rev.* B **70** 125321
[21] Bena C and Balents L 2004 *Phys. Rev.* B **70** 245318
[22] Xing Y X *et al* 2004 *Phys. Rev.* B **70** 245324
[23] Chen Z *et al* 2004 *Appl. Phys. Lett.* **85** 2553
[24] Foros J *et al* 2005 *Phys. Rev. Lett.* **95** 016601
[25] Cota E *et al* 2005 *Phys. Rev. Lett.* **94** 107202
[26] Zwierzycki M *et al* 2005 *Phys. Rev.* B **71** 064420
[27] Blaauboer M and Fricot C M L 2005 *Phys. Rev.* B **71** 041303
[28] Sela E and Oreg Y 2005 *Phys. Rev.* B **71** 075322
[29] Governale M *et al* 2003 *Phys. Rev.* B **68** 155324
[30] Benjamin C and Citro R 2005 *Phys. Rev.* B **72** 085340
[31] Thouless D J 1983 *Phys. Rev.* B **27** 6083
Niu Q 1990 *Phys. Rev. Lett.* **64** 1812
[32] Brouwer P W 1998 *Phys. Rev.* B **58** R10135
[33] Switkes M *et al* 1999 *Science* **283** 1905
[34] Wei Y D *et al* 2000 *Phys. Rev.* B **62** 9947
[35] Avron J E *et al* 2000 *Phys. Rev.* B **62** R10618
[36] Levinson Y *et al* 2001 *Physica* A **302** 335
[37] Moskalets M and Buttiker M 2001 *Phys. Rev.* B **64** 201305
[38] Wang J *et al* 2001 *Appl. Phys. Lett.* **79** 3977
[39] Vavilov M G *et al* 2001 *Phys. Rev.* B **63** 195313
[40] Wei Y D *et al* 2001 *Phys. Rev.* B **64** 115321
[41] Wang J and Wang B G 2002 *Phys. Rev.* B **65** 153311
[42] Wang B G *et al* 2002 *Phys. Rev.* B **65** 073306
[43] Moskalets M and Buttiker M 2002 *Phys. Rev.* B **66** 035306
[44] Zhu S L and Wang Z D 2002 *Phys. Rev.* B **65** 155313
[45] Wang B G and Wang J 2002 *Phys. Rev.* B **66** 125310
[46] Wei Y D and Wang J 2002 *Phys. Rev.* B **66** 195419
[47] Bychkov Y A and Rashba E I 1984 *J. Phys. C: Solid State Phys.* **17** 6039
[48] Dresselhaus G 1955 *Phys. Rev.* **100** 580
[49] Tans S J *et al* 1997 *Nature* **386** 174
[50] Frank S *et al* 1998 *Science* **280** 1744
[51] Tsukagoshi K *et al* 1999 *Nature* **401** 572
[52] Cobden D H *et al* 1998 *Phys. Rev. Lett.* **81** 681
[53] Yao Z *et al* 1999 *Nature* **402** 273
[54] Morpurgo A F *et al* 1999 *Science* **286** 263
[55] Mehrez H *et al* 2000 *Phys. Rev. Lett.* **84** 2682
Mehrez H *et al* 2001 *Phys. Rev.* B **63** 245410
[56] Roland C *et al* 2000 *Phys. Rev. Lett.* **84** 2921
Roland C *et al* 2000 *Surf. Rev. Lett.* **7** 637
[57] Orlikowski D *et al* 2001 *Phys. Rev.* B **63** 155412
[58] Datta S and Anantram M P 1993 *Phys. Rev.* B **45** 13761
[59] Tian W, Datta S and Hong S 1998 *J. Chem. Phys.* **109** 2874
[60] Taylor J, Guo H and Wang J 2001 *Phys. Rev.* B **63** 121104

[61] Blase X *et al* 1994 *Phys. Rev. Lett.* **72** 1878
Krotov Y A *et al* 1997 *Phys. Rev. Lett.* **78** 4245
Chico L *et al* 1996 *Phys. Rev. Lett.* **76** 971
Crespi V H *et al* 1997 *Phys. Rev. Lett.* **79** 2093
Chico L *et al* 1996 *Phys. Rev. Lett.* **81** 1278
Chico L *et al* 1996 *Phys. Rev.* B **54** 2600
[62] Bockrath M *et al* 1999 *Nature* **397** 598
[63] Moskalets M and Buttiker M 2002 *Phys. Rev.* B **66** 205320
[64] Wu J L *et al* 2002 *Phys. Rev.* B **66** 205327
[65] Brown E R *et al* 1991 *Appl. Phys. Lett.* **58** 2291
[66] Rosenblatt S 2005 *Appl. Phys. Lett.* **87** 153111
[67] Hirsch J E 1999 *Phys. Rev. Lett.* **83** 1834
[68] Meier F and Loss D 2003 *Phys. Rev. Lett.* **90** 167204
Sun Q F *et al* 2004 *Phys. Rev.* B **69** 054409
[69] Folk J A *et al* 2003 *Science* **299** 679
[70] Zutic I *et al* 2004 *Rev. Mod. Phys.* **76** 323